Using a Molecular Stopwatch to Study Particle Uptake in Pickering Emulsions

LANGMUIR

Article

pubs.acs.org/Langmuir

Using a Molecular Stopwatch to Study Particle Uptake in Pickering Emulsions

Joe Forth* and Paul. S. Clegg

School of Physics and Astronomy, University of Edinburgh, James Clerk Maxwell Building, Edinburgh EH9 3FD, United Kingdom

Supporting Information

ABSTRACT: Colloidal PMMA particles and an interfacially assembled, pH-switchable lipid film (tetradecylammonium hydrogen phosphate, TAHP) were combined to form emulsion droplets with composite interfaces. Two time scales govern the interfacial structure and droplet size of the system: the rate of particle adsorption and the rate of film assembly. We tune these two time scales by varying the particle size (in the case of the particles) and aqueous pH (in the case of the lipid film). Three rates of film assembly are studied: rapid (pH 5), slow (pH 7), and inactive (pH 9). At pH 5, small droplets coated with a mixed interfacial structure are formed, and increasing particle volume fraction does not change the droplet size. At pH 7, the slowed kinetics of TAHP film assembly results in the particle size having a systematic effect upon droplet size: the smaller the particles, the smaller the droplets. At pH 9, TAHP plays no role in the system, and more familiar Pickering emulsions are observed. Finally, we show that at pH 5 both the interfacial particle density and droplet size can be readily tuned in our system. This suggests potential applications in the rational design of capsules and emulsion droplets with tunable interfacial structure.

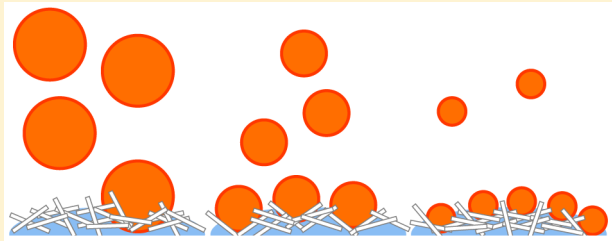

INTRODUCTION

Pickering emulsions are nonequilibrium mixtures of oil and water in which phase separation of the fluids is arrested by the addition of colloidal particles.[1−3] These particles are nearly irreversibly bound to the fluid−fluid interface by their large capillary energy, which is often on the order of $10^6 k_B T$.[4,5] These systems were discovered over a century ago; however, the last two decades have seen a significant surge in the study of their behavior. This is motivated to a great degree by a wealth of applications in the personal care, minerals, and food sectors[6,7] as well as their importance to fundamental science.[8−10] The principles of Pickering emulsion formation are fairly well understood;[11] however, to fully realize their potential, a number of open questions must be answered.

Of particular interest is the effect of particle size upon the time scale of particle adsorption onto the oil−water interface and how this affects the droplet size in the resulting emulsion.[12] Direct studies of adsorption in Pickering emulsions are scarce, but the theory of the rate of particle adsorption onto the liquid−gas interface has been extensively studied in the context of froth flotation. Despite a number of complicating factors,[13−15] a qualitative understanding of the system can be developed solely by considering hydrodynamics, diffusion, and particle size.[16] For large particles (radius, $r \gtrsim 5$ μm), hydrodynamics alone predicts that particle adsorption rates increase with r.[17] For small particles ($r \lesssim 5$ μm), the consideration of diffusive motion predicts enhanced adsorption of particles with decreasing r.[18,19] Despite the importance of understanding kinetic effects in emulsion formation, systematic studies looking at analogous phenomena in Pickering emulsions are lacking.

The use of a molecular emulsifier in tandem with colloidal particles can provide insight into kinetic effects in Pickering emulsions.[20] The second emulsifier introduces a second, much shorter time scale, that of adsorption of the molecular component.[12,21] Adding a molecular component to a Pickering emulsion is thought to retard droplet coalescence, giving the particles more time to adsorb and leading to reduced droplet size.[22] Pichot and Norton observed this using emulsions stabilized by silica particles and monoolein. Under the conditions studied, monoolein alone was found to confer only short-term stability to emulsions. However, increasing the concentration of monoolein in silica-stabilized oil-in-water emulsions led to a systematic reduction in droplet size that lasted several months.[22] This paradigm was also recently used by Thijssen to interpret the reduction in droplet size that the addition of Rhodamine B (a fluorescent dye) led to in Pickering emulsions.[23]

In this work, we systematically study emulsions stabilized by a composite interface. We use two emulsifiers: colloidal particles and an interfacially assembling lipid, which we have characterized recently.[24] The lipid consists of tetradecylamine (initially dispersed in dodecane) and hydrogen phosphate (initially dissolved in water). The amine and the salt bind stoichiometrically to one another at the oil−water interface,

Received: April 18, 2016
Revised: June 10, 2016
Published: June 10, 2016

DOI: 10.1021/acs.langmuir.6b01474
Langmuir 2016, 32, 6387−6397

forming tetradecylammonium phosphate (TAHP). The rate at which TAHP coats the droplets can be tuned, from rapid (at pH 5) to slow (at pH 7) to inactive (at pH 9). We study particles of radius 500, 726, and 990 nm. This size range probes a region in which diffusive effects become more significant as particle size decreases and is of great importance to both Pickering emulsion stabilization and the theory of particle adsorption rates.[16] By adding two components that both compete for the oil−water interface, the effective time scales of these two emulsification mechanisms can be compared. By tuning the time scale of TAHP formation, we systematically study how rapidly particles are prevented from adsorbing onto the oil−water interface. We infer this from a change in droplet size, which we find systematically depends on the particle size and hence the particle adsorption rate. We also find that using these two emulsifiers in combination gives us control over a wide range of values of a number of important parameters. Droplet size, particle area density, and interfacial film structure (including its effective dimensionality) can all be readily controlled in our system.

EXPERIMENTAL SECTION

Sterically Stabilized Colloidal PMMA. Colloidal poly(methyl methacrylate) (PMMA) particles with radii of 500, 726, and 990 nm were synthesized by dispersion polymerization and characterized by dynamic light scattering. The particles were sterically stabilized by covalently grafting poly-12-hydroxystearic acid (PHSA) chains onto the particle surface. 7-Nitrobenzo-2-oxa-1,3-diazol (NBD-Cl, Sigma-Aldrich) was covalently bonded to the PMMA polymer backbone to yield fluorescent particles.[25] A second dye, 1,1′-dioctadecyl-3,3,3′,3′-tetramethylindocarbocyanine perchlorate ($DiIC_{18}$, Sigma-Aldrich), was used to dye PMMA particles of radius 760 nm. This was done to allow for fluorescence signal separation from the colloidal PMMA and NBD-doped tetradecylamine.[26] To ensure identical sample history, all particles were washed 10 times in hexane, after which they were dried overnight in a vacuum oven at 40 °C. Dispersions of colloidal PMMA in dodecane of a known particle volume fraction, ϕ, were then formed by dispersing a measured mass of the particles in dodecane and dispersing thoroughly using an ultrasonic bath and sample shaker for a week. This yielded particle dispersions of ϕ = 0.1 that consisted predominantly of single particles, with only a small number of residual doublets, triplets, and particle oligomers found to remain in the sample.

Colloidal particle volume fractions added to the emulsions (measured as a volume fraction of the oil phase) were selected such that particle dispersions of all radii would occupy equal cross-sectional areas, S, per unit volume. Assuming equal contact angles for all particle radii, this is given by

$$S = \frac{3\alpha\phi}{4r_p} \tag{1}$$

where α is the oil/water volume ratio (4 throughout this work) and r_p is the particle radius. Three particle volume fractions, referred to as low (ϕ_{low}), intermediate (ϕ_{mid}), and high (ϕ_{high}) throughout this work, are given in Table 1. These three particle volume fractions were chosen for the three differing regimes of emulsification they lead to. These three regimes are discussed in the Supporting Information (Figures S1 and S2).

Table 1. Particle Volume Fractions (ϕ) That Stabilize Identical Quantities of Emulsion Surface Area, Compared for the Radii of Particles (r_p) Used in This Work

r_p (nm)	ϕ_{low}	ϕ_{mid}	ϕ_{high}
500	0.00068	0.0048	0.025
726	0.0010	0.0070	0.037
990	0.0014	0.0095	0.050

Emulsion Preparation. The aqueous phase contained 100 mM phosphate ions at pH 5, 7, and 9. Phosphate buffer solutions were prepared using appropriate ratios of sodium phosphate salts ($NaH_2PO_4{\cdot}H_2O$ and $Na_2HPO_4{\cdot}2H_2O$, ≥99%, Sigma-Aldrich), and small adjustments to pH were made using 1 M solutions of NaOH and phosphoric acid. Differentiation of the continuous and the dispersed phase was achieved by adding a small quantity (<1 mg/20 mL) of Nile red (a water-insoluble fluorophore, technical grade, Sigma-Aldrich) to dodecane and imaging the system using fluorescence confocal microscopy. Fluorescence imaging of the TAHP film was achieved by doping the system with 4-chloro-7-nitrobenzofurazan (NBD-Cl, 98%, Sigma-Aldrich), which binds covalently to the primary amine.[27] NBD-Cl was used as obtained, and a small quantity of it (≤2 mg/20 mL) was dispersed in the phosphate solutions using an ultrasonic bath for several hours. Samples were then filtered using a Millex syringe-driven poly(ether sulfone) filter unit with a pore size of 200 nm. Use of the resulting solution led to the formation of emulsions qualitatively identical to those formed without NBD. Dodecane (ReagentPlus, ≥99%) and tetradecylamine (TDA, ≥95%) were purchased from Sigma-Aldrich and used as obtained. Emulsions were prepared using 1 mL of aqueous solution and 4 mL of dodecane. Prior to emulsification, the TDA and colloidal PMMA were dispersed in the dodecane, and the phosphate salts and NBD-Cl were dissolved in the aqueous phase. Emulsions were formed by shear using a Polytron PT-3100 rotor/stator (Kinematica) with a 5-mm-diameter attachment. The gap between the rotor and the stator was 0.15 mm, and emulsification was performed for 1 min at a shear rate of 24 000 s^{-1}.

Droplet Sizing. Droplet sizing was performed using a Beckmann-Coulter LS 13320 single-wavelength laser diffraction particle size analyzer. Approximately 10 μL of emulsion was dispersed in 10 mL of dodecane, and the samples were then illuminated using a 5 mW 780 nm laser. The wavelength of the laser is sufficiently long that the contribution to the scattering signal from NBD fluorescence was negligible. During sizing, samples were agitated by a magnetic stirring bar to prevent sedimentation. The sparing solubility of TAHP in dodecane at room temperature led to the coalescence of samples, so measurements were performed in a weak (1 mM) dispersion of tetradecylamine in dodecane to suppress this effect. In the case of the emulsions containing large particles (r_p = 990 nm), the particles were detected by the sizer, leading to an erroneously high estimate of the specific surface area of the resulting emulsion. Specific surface areas of all emulsions were therefore calculated using particle size distributions truncated to exclude particles of diameter smaller than 3.5 μm, which was significantly smaller than any droplets observed in this work. Mean droplet diameters are reported in terms of the de Brouckere mean diameter, d_{43}. For N droplets, this is defined as

$$d_{43} = \frac{\sum_i^N d_i^4}{\sum_i^N d_i^3} \tag{2}$$

Sample Imaging. Fluorescence confocal micrographs were obtained using a Zeiss LSM T-PMT/LSM700 confocal laser scanning inverted microscope with Zeiss ZEN software (Carl Zeiss AG, Germany). Both air (10× and 20× magnification, NA = 0.3 and 0.4, respectively) and oil-immersion objectives (40× magnification, NA = 1.3) were used to image the samples. Samples were held in custom-made imaging chambers that consisted of a 7 mL glass vial with the base removed. The vials were then attached to a ground glass coverslip using Norland 61 UV-setting optical adhesive. Sealed imaging chambers were heat-hardened in an oven at 50 °C for at least 5 days prior to use to prevent dissolution of the optical adhesive into the dodecane.

RESULTS AND DISCUSSION

We begin by discussing some properties of TAHP as an emulsifier before combining it with colloidal PMMA to produce droplets with composite interfaces. The lipid film used in this

DOI: 10.1021/acs.langmuir.6b01474
Langmuir 2016, 32, 6387−6397

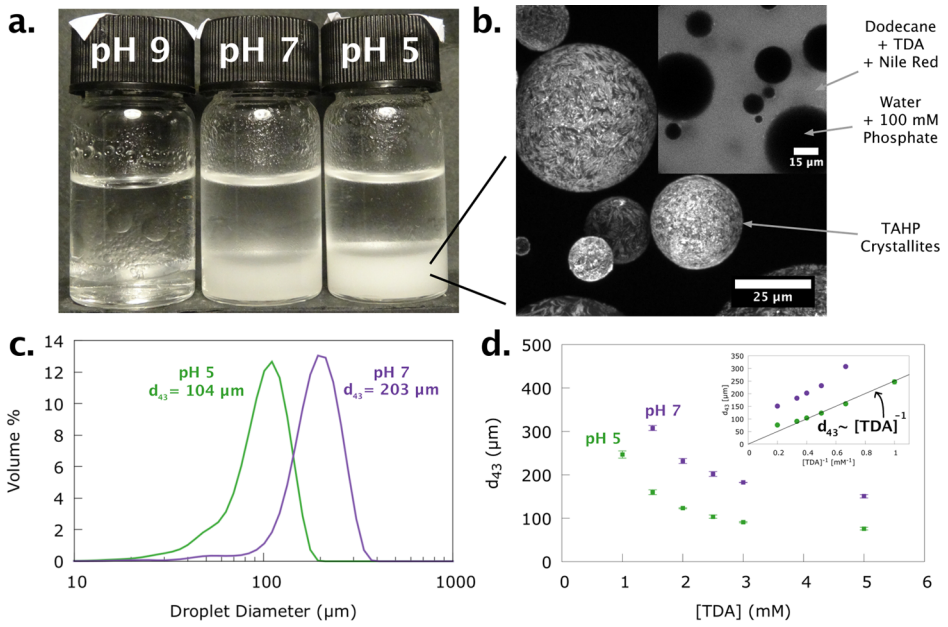

Figure 1. (a) TAHP-stabilized water-in-oil emulsions over a range of pH values. (b) Confocal micrographs of the resulting emulsion in which TAHP has been doped with NBD and (inset) Nile red has been added to dodecane. (c) Droplet size distributions for [TDA] = 2.5 mM with aqueous pH 5 (green) and 7 (purple). (d) de Brouckere mean droplet diameters at pH 5 and 7 for [TDA] are between 1 and 5 mM. (d, inset) d_{43} vs $[TDA]^{-1}$ for pH 5 and pH 7, along with a linear fit to the data at pH 5. Error bars show the standard deviation in the mean of three measurements.

work is rather novel. It consists of two components—(oil-insoluble) hydrogen phosphate and (water-insoluble) tetradecylamine (TDA)—that are initially separated in immiscible phases. Bringing TDA-containing dodecane and hydrogen phosphate-containing water into contact with one another below a critical pH (approximately 8.5) leads to the condensation of HPO_4^{2-} at the positively charged fatty amine monolayer. This leads to the formation of thick, interfacial films of tetradecylammonium phosphate (TAHP) crystallites with a well-defined stoichiometry. We have investigated many aspects of its behavior recently.[24] The most important feature of its behavior to this work is the pH-tunable rate at which TAHP forms, which varies from rapid (pH 5) to slow (pH 7) to inactive (pH 9).

TAHP-Stabilized Emulsions. TAHP-stabilized water-in-oil emulsions over a range of aqueous pH values are shown in Figure 1a. Three regimes of emulsification (and hence TAHP formation) can be observed. At pH 5 and 7, a water-in-oil emulsion that is highly stable against coalescence has been formed. At pH 9, TAHP has been rendered ineffective as a stabilizer, and the two fluids rapidly phase separate. Fluorescence confocal micrographs of the emulsion formed at pH 5 are shown in Figure 1b, in which the TAHP film has been doped with NBD-Cl. This produces fluorescent TAHP crystallites, which can be clearly distinguished in the image. The Figure 1b inset shows TAHP-stabilized emulsions in which Nile red, a hydrophobic fluorophore, has been added to dodecane. This shows that this is a water-in-oil emulsion. Droplet diameter distributions, measured using a laser diffraction particle sizer, are shown for a TDA concentration ([TDA]) of 2.5 mM in Figure 1c at pH 5 (green) and pH 7 (purple). The droplet size doubles as the pH is increased from 5 to 7, while [TDA] is kept constant. Emulsions formed under all conditions had a single primary droplet diameter and a polydispersity of approximately 30%.

Figure 1d shows the de Brouckere mean droplet diameter (d_{43}) plotted against [TDA] and (inset) $[TDA]^{-1}$. The average droplet diameter exhibits a power-law dependence on the initial concentration of TDA added to the system. At pH 5, data points at all except the highest TDA concentration ([TDA] = 5 mM) are inversely proportional to one another ($d_{43} \approx [TDA]^{-1}$). Increasing the pH to 7 results in a deviation from this behavior. The droplet size measurements are highly repeatable, with the standard deviation in the mean of d_{43} typically ±5% or less, showing that TAHP can be used to achieve a high degree of control over droplet size.

The change from pH 7 to pH 9 renders the TAHP ineffective as a stabilizer. This is because the fatty amine is no longer charged at the oil−water interface and has a significantly reduced surface activity, above pH 8.[28,29] The effect of this in our system is to reduce the quantity of TAHP formed, which we have shown in previous work decreases to zero at pH 9.[24] Between pH 5 and 7, the amount of TAHP formed is known to be constant: as there is a large excess of phosphate in the system, at least 90% of the TDA is converted to TAHP. However, the rate at which TAHP forms is significantly retarded when the pH is increased from 5 to 7.[24]

We must also address here the differing droplet size between pH 5 and 7. The formation of stable Pickering emulsions (shown in Supporting Information, Figure S1) with a smaller radius compared to that of the TAHP-stabilized emulsions presented in Figure 1 means surface tension effects during droplet breakup can be ruled out, as surface tension will be reduced by the presence of the amine.[29] Although the amount of TAHP formed is identical at pH 5 and 7,[24] it may be that less TAHP is formed on the shorter time scale of emulsification at pH 7. This can be investigated by emulsifying the system for longer times. If the amount of TAHP formed were kinetically limited, then extending the amount of time for which the system was sheared would result in a smaller drop size. Curiously, shearing the pH 7 system for 10 min (rather 1)

DOI: 10.1021/acs.langmuir.6b01474
Langmuir 2016, 32, 6387−6397

yielded slightly larger rather than smaller droplets (an increase in d_{43} from 203 to 245 μm). This suggests that prolonged mechanical stresses do indeed lead to the TAHP crystallites detaching from the droplet interface, as has been observed in Pickering emulsions.[30] In our previous work, we also showed that the TAHP crystallite size increases with pH.[24] Larger crystallites would result in a thicker interfacial monolayer. Furthermore, larger crystallites with lengths on the order of 10 μm would be unlikely to adsorb onto the curved surface of smaller droplets. It therefore seems likely that the increased droplet size at pH 7 is due to both the detachment of crystallites during shear and increased crystallite size, though we do not investigate the effect further here.

Varying Particle Radius in Composite Interface Emulsions. Colloidal PMMA was then added to the dodecane prior to emulsification. Alone, PMMA and TAHP both stabilize water-in-oil emulsions. Some of the features of PMMA-stabilized emulsions have been discussed in the Supporting Information (Figures S1 and S2). By varying the radius of the PMMA particles, the rate of particle adsorption was varied. This results in there being two tunable time scales governing emulsification: particle adsorption and TAHP formation. The effect of varying these two time scales upon the resulting emulsion was initially studied at pH 5 and 7, r_p = 500, 726, and 990 nm, using drop size measurements and fluorescence confocal microscopy. Particle volume fractions are adjusted such that they can coat an equal amount of cross-sectional area (equivalent to ϕ = 0.007 at r_p = 726 nm; details given in Table 1 in the Experimental Section). All samples contained 2.5 mM TDA prior to emulsification.

At pH 5, the addition of the PMMA particles makes a negligible difference in the droplet size for r_p = 726 and 990 nm. The addition of r_p = 500 nm particles leads to a slight reduction in d_{43} from 104 to 84 μm, which is reflected in a shift of the droplet size distribution. At pH 7, the addition of colloidal PMMA leads to a significant reduction in droplet diameter, which occurs for all particle radii. Importantly, the reduction in droplet diameter depends systematically on the radius of the particles used. The smaller the particles are, the greater the reduction in droplet diameter. At pH 7, d_{43} with no added particles is 202 μm. This decreases to 154 μm for r_p = 990 μm (the smallest change observed), 128 μm for r_p = 726 nm, and 117 μm for r_p = 500 nm. The polydispersity of the droplets is approximately 40% for all of the emulsions studied here. The droplet size distributions are dominated by a primary maximum in droplet size, with a second, much smaller shoulder or secondary peak detected in some of the emulsions formed at pH 7. Droplet size distributions for ϕ_{mid} at pH 5 (blue lines) and 7 (orange lines) are shown in Figure 2a. A control experiment, in which an emulsion stabilized with 2.5 mM TDA alone, is also shown (darkest lines). d_{43} vs r_p for both pH 5 and 7 is shown in Figure 2b. At pH 7, the specific surface area of the droplets occupied by the particles, S_p, could be plotted against $r_p^{-2/3}$ to give the roughly linear trend shown by the line in Figure 2c.

The systematic dependence of droplet size on particle size and pH can be understood as a result of the interplay between particle adsorption rates and TAHP formation rates. TAHP coats the droplets in a thick, elastic film of TAHP crystallites, which inhibits particle adsorption. This puts an effective upper limit on the time scale on which the PMMA particles can adsorb onto the interface. By increasing the pH, the particles are given more time to adsorb onto the surface of the droplet.

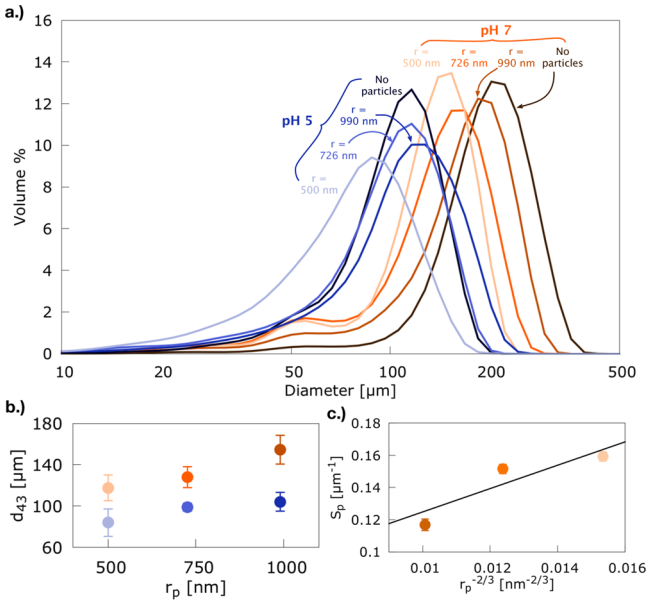

Figure 2. (a) Droplet size distributions of emulsions stabilized by a composite TAHP/PMMA interface. (b) d_{43} values at pH 5 and 7 for all particle radii. (c) Specific surface area occupied by the particles, S_p, vs$r_p^{-2/3}$ for pH 7 data. The aqueous phase is at (blue) pH 5 and (orange) pH 7. r_p = 990, 726, and 500 nm. [TDA] = 2.5 mM. A control experiment with no extra particles is also shown (darkest line). The particle radius is indicated by the depth of color, with smaller particles assigned lighter line colors. Error bars show the standard deviation in the mean of three measurements.

Clearly at pH 5 the TAHP layer forms more quickly than the characteristic adsorption time of even the smallest particles, so there is no particle size dependence of the droplet size. However, at pH 7 it appears that the TAHP layer formation time and the particle adsorption times are much more similar.

A consideration of the hydrodynamics of the system during emulsification, along with the relative importance of flow-driven and diffusive mass transfer, allows this concept to be developed further. The nature of the flow within the shear gap of the rotor-stator is described by the Reynolds number, *Re*, where[21]

$$Re = \frac{vl\rho}{\eta} \tag{3}$$

For a rotor-stator with a tip velocity v, a rotor-stator gap l, a continuous phase viscosity η, and a continuous phase (dodecane) density ρ, *Re* is approximately 300, and laminar flow is anticipated in the shear gap. In the laminar flow regime, the mass transfer of particles, the size of the droplet, and the size of the particles can be related.[18] The relative importance of hydrodynamic versus diffusive motion can be estimated from the Péclet number, *Pe*,

$$Pe = \frac{2r_d u_d}{D_p} \tag{4}$$

where r_d and u_d are the radius and velocity of the droplet, respectively. D_p is the diffusion coefficient for particles of radius r_p in a fluid of viscosity η and is given by the familiar Stokes–Einstein relation $D_p = \frac{k_B T}{6\pi\eta r_p}$, where k_B is the Boltzmann constant and T is the absolute temperature. Given a difference in flow rates of 1 m s^{-1} across a 100-μm-diameter droplet within the shear gap, the Péclet number in the system will be as

DOI: 10.1021/acs.langmuir.6b01474
Langmuir 2016, 32, 6387–6397

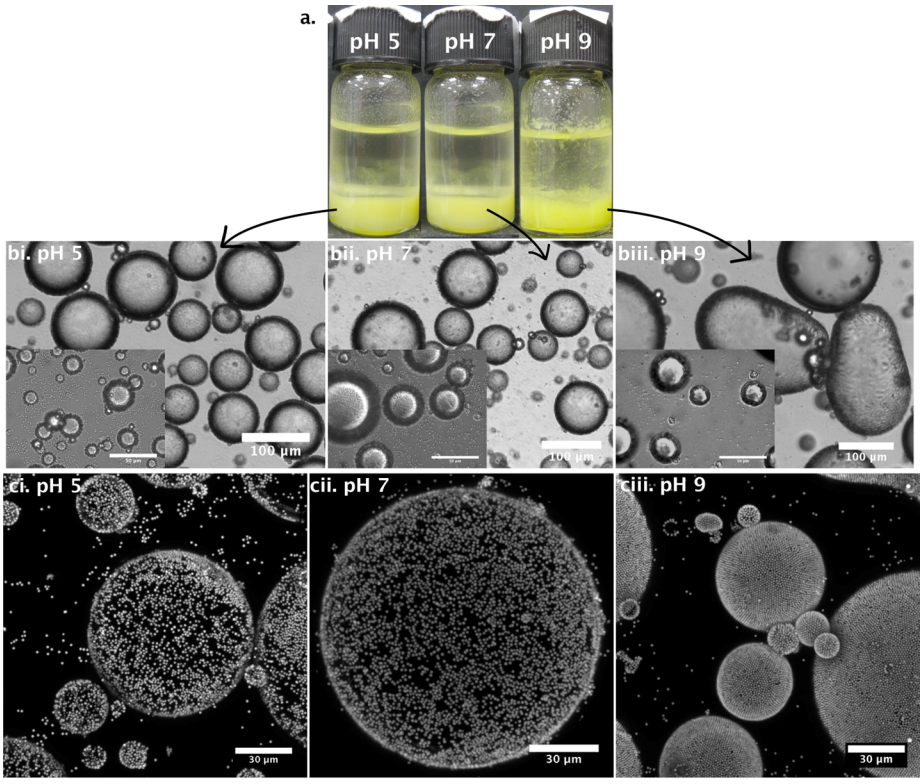

Figure 3. (a) Photographs and (b) light micrographs of TAHP/PMMA-stabilized emulsions containing an aqueous phase at pH 5 (i), 7 (ii), and 9 (iii). (Inset) High-magnification micrographs showing residual particles in the supernatant. (c) Fluorescence confocal micrographs showing the fluorescence signal from the colloidal PMMA particles (white). ϕ = 0.007 (= ϕ_{mid}), r_p = 726 nm, and [TDA] = 2.5 mM. The emulsions shown here are identical to those in Figure 1b, albeit with PMMA particles added to dodecane prior to emulsification.

high as 10^9. This means that the laminar flow driven by the rotor-stator dominates the thermal diffusion of the particles.

Because of its relevance to froth flotation phenomena, the relationship among bubble size, particle size, and particle adsorption time has been the subject of study for decades.[31,32] Froth flotation research explicitly studies the adsorption of particles from a liquid onto a gas bubble; however, we believe that the enhanced particle adsorption for smaller particles shown in Figure 2a occurs as a result of a similar mechanism. The number of particles that adsorb onto the surface of a droplet, N_{ads}, relative to the number of particles through which the droplet flows, N, is related to the Péclet number by[18]

$$\frac{N_{ads}}{N} = 4fPe^{-2/3} \tag{5}$$

where f describes the tendency of a particular particle to adsorb onto the droplet surface and is between 0 and 1.[18,19,21] To model this, we assume that particle adsorption in the emulsion droplets happens before the elastic TAHP film forms. On these short time scales, the droplet size is governed by surface tension rather than interfacial elasticity. After the system has coarsened via limited coalescence, the composite interface consists of a fixed amount of TAHP and a number of particles that depends on r_p. The amount of specific surface area occupied by the particles, S_p, is expected to scale with r_p as

$$S_p = S_{total} - S_{TAHP} \approx r_p^{-2/3} \tag{6}$$

where S_{total} is the total specific surface area of the emulsion and S_{TAHP} is the specific surface area of a particle-free emulsion. (This expression is derived from eq 5 and the definition of the Péclet number in the Supporting Information.) Calculating S_{total} from the pH 7 data in Figure 2a and plotting S_p against $r_p^{-2/3}$ gives reasonable agreement with this trend over the range of particle sizes studied here, as shown in Figure 2c. This shows that the relatively small particles studied here are in the diffusion-enhanced adsorption regime and that the probability of the particles adsorbing, f, does not change strongly across the different particle sizes.

Studying this system during emulsification limits our ability to make truly quantitative statements about particle adsorption kinetics; however, a number of observations can still be made. In our previous work, we showed that at pH 7 a 1-mm-diameter droplet was coated in a rigid TAHP shell in under 5 s by diffusion-limited TAHP formation.[24] For the ~100-μm-diameter droplets studied here, the interfacial dynamics will be arrested more rapidly because of both the presence of mixing flow and the greater surface area available for TAHP formation. This means that the diffusion of the particles at the interface will be negligible prior to interfacial arrest. Furthermore, the particles at the interface are irreversibly adsorbed. Such a system is most reminiscent of the random sequential adsorption (RSA) models of adsorption kinetics, which describe the probability of adding a randomly located sphere or disk to an existing configuration.[33] In this model, the characteristic adsorption time of the particles, τ_a, is expected to be inversely proportional to the particle volume fraction, ϕ. It would be expected, therefore, that the concentration of particles adsorbed at the interface would increase with increasing ϕ. We show qualitatively that this is the case in Figure 5 and even find that the addition of a very large quantity of particles results in the interface being coated in TAHP-PMMA particle aggregates.

DOI: 10.1021/acs.langmuir.6b01474
Langmuir 2016, 32, 6387−6397

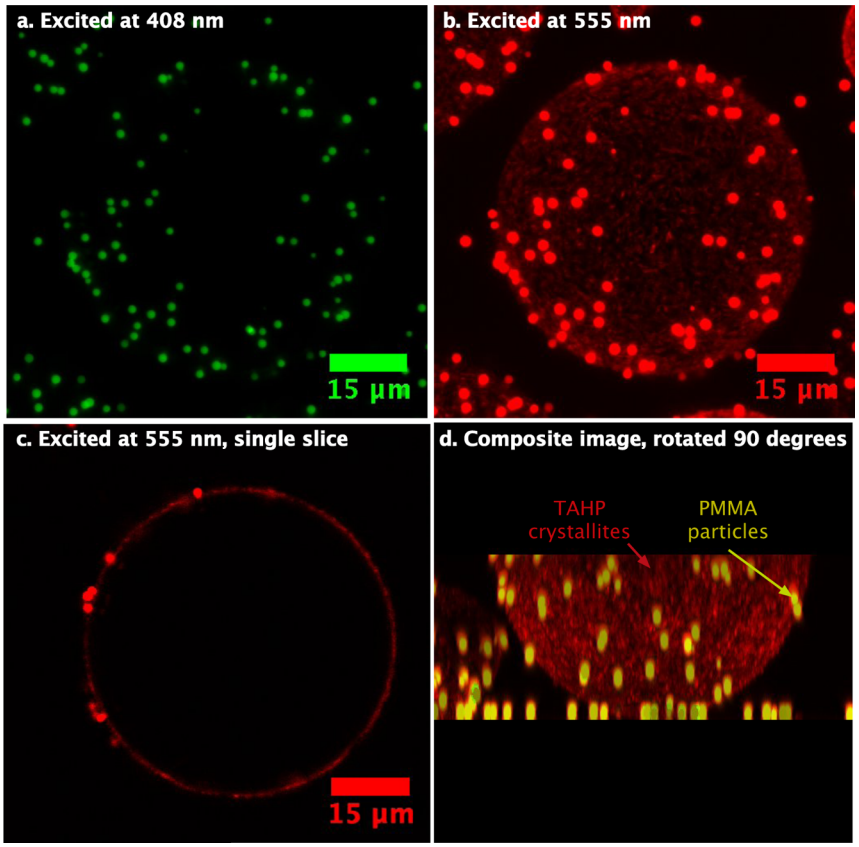

Figure 4. Fluorescence confocal micrograph showing water droplets in dodecane stabilized by a composite interfacial film that consists of TAHP and colloidal PMMA. Illumination at two different wavelengths [(a) 408, (b) 555 nm] shows fluorescence signals from both the NBD-dyed colloidal PMMA and the NBD-doped TAHP. (c) Single slice, excited at 555 nm, with the focal plane approximately at the droplet equator. (d) 3D projection of the two fluorescence signals, rotated 90° around the image plane.

We will also show later, in Figure 6, that at pH 5 the size of the droplets is, for the most part, determined by the tetradecylamine concentration, allowing us to tune the particle density.

A number of other effects may also play a role in this system's behavior. Interactions between TAHP and PMMA are likely to yield behavior more complicated than that predicted by eq 6, such as due to the formation of TAHP-PMMA aggregates. The particle size dependence of the droplet diameter may be complicated by the smaller particles adsorbing at the interstices between TAHP crystallites. These factors are all strongly dependent on the structure of the interface, which we study in the following sections. A third issue is that the particle volume fraction may be insufficient to alter the diameter of the smaller ([TDA] = 2.5 mM, pH 5) droplets and that simply adding more particles would lead to a reduction in d_{43}. We tackle this explicitly later, in which we use larger droplets formed at pH 5, [TDA] = 1.25 mM, and show that the droplet diameter is independent of the particle volume fraction for an order of magnitude in ϕ.

Tuning Interfacial Structure via pH. Aside from varying the droplet size, tuning the efficacy and kinetics of action of the two emulsifiers was also found to control the interfacial structure of the emulsions. We investigate this in the following sections. We also show a pH-dependent synergy between the emulsifiers, in which the PMMA particles result in the formation of an emulsion even at pH 9, when TDA is no longer an effective emulsifier.

Photographs of emulsions stabilized by the TAHP/PMMA film at pH 5, 7, and 9 are shown in Figure 3a. At pH 5 and 7, the emulsions are identical. The droplet−oil boundary is smooth, suggesting that there are no multidroplet aggregates. There is no excess water, showing that it has all been emulsified. At pH 9, the macroscopic appearance of the emulsion changes radically. The addition of colloidal PMMA has led to the formation of a stable emulsion at pH 9, whereas in the presence of TAHP alone no stable emulsion was formed. The droplet−oil boundary is rough, and a visual inspection of the emulsion formed at pH 9 showed large fractal aggregates of droplets.

Light micrographs comparing the appearance of the emulsions are shown in Figure 3b. High-magnification micrographs are also used to show the residual particles remaining in the dodecane supernatant (Figure 3b, inset). The light micrographs show a trend similar to that in the photographs. The emulsions formed at pH 5 and pH 7 are qualitatively very similar. The majority of the droplets are spherical, and a significant number of particles have remained in the supernatant. At pH 9, the appearance of the system changes greatly: the droplet size has increased significantly, and the majority of the droplets are nonspherical. An inspection of the supernatant in the Figure 3biii inset also shows a vastly reduced number of PMMA particles in the supernatant at pH 9. Droplet stability against coalescence was not fully studied in this work, at least in part because no significant coarsening or coalescence of the droplets was observed in any of the samples during the course of the study (2 years).

Finally, Figure 3c shows fluorescence confocal micrographs that show the fluorescence signal from the particles alone. They

DOI: 10.1021/acs.langmuir.6b01474
Langmuir 2016, 32, 6387−6397

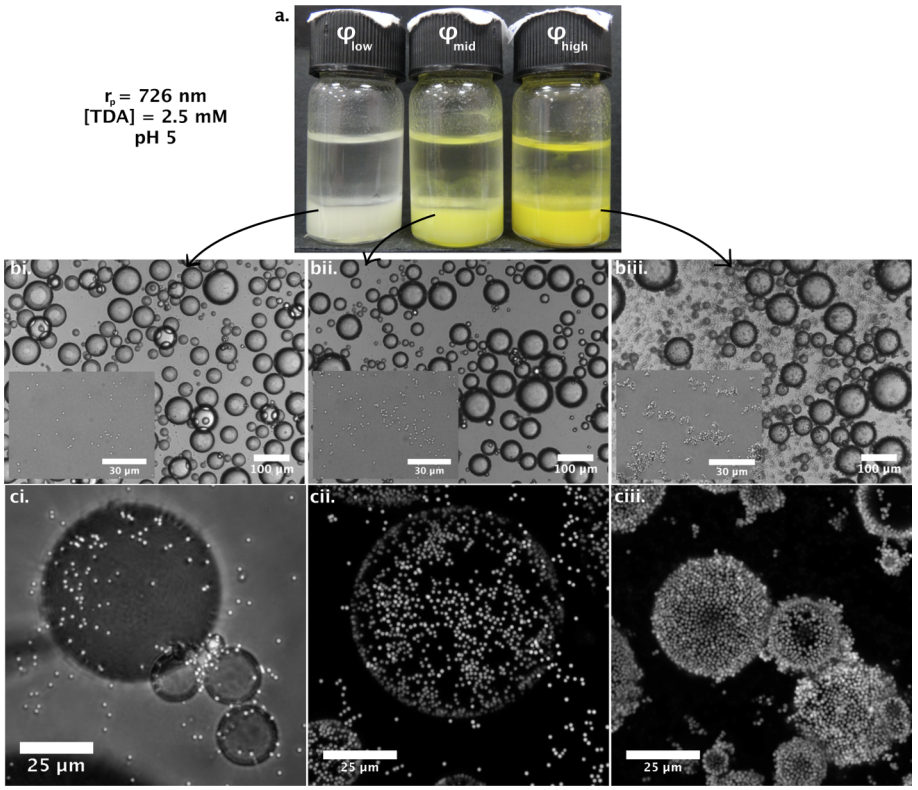

Figure 5. (a) Photographs, (b) light micrographs, and (c) fluorescence confocal micrographs of composite interface emulsions at increasing (l–r) ϕ and constant r_p. (b, inset) High-magnification light micrographs of the supernatant of each emulsion. r_p = 726 nm, [TDA] = 2.5 mM, and pH 5.

corroborate the trends in Figure 3a, b. At pH 5 and 7, the appearance of the system is similar. The droplet interface appears patchy. Only the PMMA particles contain a fluorophore in these images. It can therefore be inferred that the droplets at pH 5 and 7 have a partial coating of particles. In spite of this, these droplets are very stable against coalescence. Particles can been seen both at the droplet interface and in the supernatant. Particles were not observed to move during the 2 h for which the system was observed, suggesting that something is arresting their thermal motion. At pH 9, the droplets look like more-familiar Pickering emulsions: the patches seen at pH 5 and 7 are absent. Figure 3ciii shows a confocal z stack of a multidroplet aggregate formed at pH 9. A single slice of such an aggregate, shown in a system with larger particles in the Supporting Information (Figure S5), shows that these aggregates contain particles that occupy the interfaces of multiple droplets simultaneously. The trends in interfacial structure shown here were seen at all pH values and particle radii studied in this work. This is shown in the Supporting Information, Figure S3.

The variation in interfacial structure in Figure 3c is due to the varying efficacy of TAHP with pH. This is not a kinetic effect such as that probed in the previous section but rather is due to the quantity of effective emulsifier decreasing as the pH is increased. At pH 9, the TDA is inactive as a stabilizer. As a result, only the colloidal PMMA coats the droplets and Pickering emulsions stabilized by a jammed particle monolayer are formed. At pH 5 and 7, both particles and TAHP must compete to occupy the droplets' surface, resulting in patchy droplets.

The absence of TAHP at pH 9 is also what leads to the change in the macroscopic appearance of the emulsion. The roughness of the boundary between the water droplets and dodecane is due to the formation of droplet aggregates. This occurs because particles occupy the surface of two droplets simultaneously, binding the droplets together. We describe our findings using the work by French et al.,[34] which points us toward two pieces of evidence that allow us to draw this conclusion. First, even in the absence of TAHP, the aggregation of the droplets is inhibited by the addition of extra colloidal particles (see Supporting Information, Figure S1a). Second, direct imaging of the aggregates using fluorescence confocal microscopy in systems at pH 9, both with and without 2.5 mM TDA added to the dodecane, shows particles being shared by droplets (Supporting Information, Figures S2 and S5). Although the particle bridging effect itself is rather fine-tuned, it is reasonable to think that it will occur in this system. The contact angle must be sufficiently high such that the particles can protrude far enough to be shared by the droplets but not so far that the capillary energy binding the particles to the interface becomes negligible. The PMMA particles used in this study have been estimated to have a contact angle of 150–160° with respect to the dodecane–water interface,[23] well within the region in which particle bridges can be expected to be found.

A number of questions remain as to the interfacial structure of the composite interface emulsions. The confocal micrographs in Figure 3 show quiescent, patchy interfaces with dark, nonfluorescent regions. The absence of particle motion and the pH dependence of the interfacial structure both suggest that this patchiness is due to the presence of TAHP crystallites at the interface. This was confirmed by tagging both PMMA and TAHP with different fluorophores. To achieve signal separation, TAHP was doped with NBD-Cl and the particles were tagged with $DiIC_{18}$.

DOI: 10.1021/acs.langmuir.6b01474
Langmuir 2016, 32, 6387–6397

The achieved signal separation is shown in Figure 4. The system was illuminated using lasers with a wavelength of 408 nm (Figure 4a, green, showing only the particles) and 555 nm (Figure 4b, red, showing both the PMMA particles and the TAHP crystallites). They show that the droplet is coated with both colloidal PMMA and TAHP crystallites. A single confocal slice taken near the droplet equator (Figure 4c) shows the rather hydrophobic PMMA particles clearly adsorbed onto the oil−water interface. Rotating the image 90° around the image plane (Figure 4d) shows that the particles are homogeneously distributed at the droplet interface and that the PMMA particles are embedded in a matrix of TAHP crystallites. The system was observed for over 1 h, during which time neither the particles nor the crystallites moved. This is because the rigid TAHP network arrests the thermal motion of the colloidal PMMA.[24]

Effect of Particle Volume Fraction on Interfacial Structure. Thus far, we have looked at the emulsions stabilized by TAHP and used these to gauge how the rate of adsorption of colloidal PMMA depends on the particle size. In the following sections, we investigate how varying the pH and particle size affects the interfacial structure of the emulsions. This serves both to investigate potential applications of the system in encapsulation and tuning interfacial structure and to address some questions raised in the discussion of results in the previous section. At pH 5, 7, and 9, the interfacial structure of the droplets at three particle volume fractions was investigated: ϕ_{low}, ϕ_{mid}, and ϕ_{high} (given in Table 1). We will show that by varying the particle volume fraction not only can the particle area density at the droplet interface be varied enormously but at very high particle volume fractions the interface acquires fractal dimensionality, with long tendrils (up to 30 μm) extending from the droplet interface. As a control experiment, PMMA-stabilized emulsions at identical volume fractions were also made (Supporting Information, Figures S1 and S2).

Emulsions stabilized by a TAHP/PMMA interface at three particle volume fractions are shown in Figure 5. The photographs in Figure 5a show emulsions that are qualitatively similar in appearance; the increasingly yellow color of the emulsions is due to the increasing particle volume fraction. The emulsion−oil boundary is smooth, suggesting that few or no aggregated droplets are present. This is confirmed in the light micrographs shown in Figure 5b. The light micrographs show droplets of a similar size for all particle volume fractions. This is even the case, surprisingly, for ϕ_{high}, which shows droplets of approximately the same size as those formed at ϕ_{low} and ϕ_{mid}.

Figure 5b, inset, shows that both the number and structure of particles in the supernatant depend on ϕ. The number of particles remaining in the supernatant increases with ϕ. At ϕ_{low} and ϕ_{mid}, these are typically present as individual particles, with a small number of multiparticle aggregates seen. At large ϕ_{high}, multiparticle aggregates are seen. These do not form in the absence of TAHP, so their presence can be directly attributed to TAHP.

The fluorescence confocal micrographs in Figure 5c show that the interfacial structure evolves with ϕ in much the same way as the arrangement of the particles in the supernatant. The density of the particles at the interface increases with ϕ. At ϕ_{low}, the majority of the interface is coated with TAHP, and only a few particles are seen on the droplet interface. Increasing the particle volume fraction to ϕ_{mid} increases the density of particles at the interface, recovering the patchy appearance of the droplets seen in Figure 3c. At both ϕ_{low} and ϕ_{high}, a single layer of PMMA and TAHP coats the droplets. At ϕ_{high}, the PMMA/TAHP aggregates that were seen in the supernatant in Figure 5b can also be seen projecting from the droplet surface in Figure 5c, giving the droplets a hairy appearance. Other images of these tendrils can be found in the Supporting Information, Figure S5. The particles at the droplet surface were not seen to move, showing that their thermal motion is arrested by the TAHP network. By contrast, the tendrils were seen to be both perturbed by subphase flows and to undergo thermal motion. The tendrils themselves did not undergo translational motion along the droplet surface, and it was thus inferred that they were anchored to the TAHP/PMMA interface.

Three regimes of interfacial structure are observed by varying ϕ. At ϕ_{low} and ϕ_{mid}, increasing particle volume fraction increases the density of particles present at the interface. This yields droplet interfaces with a sparse or patchy coating of particles. At ϕ_{high}, particle multilayers and large tendrils are seen to extend from the interface. These tendrils, which consist for the most part of aggregated PMMA particles, were also found in the dodecane supernatant of the emulsions.

The exact mechanism of the formation of these aggregates is not clear. They do not form in PMMA-stabilized Pickering emulsions formed at ϕ_{high} nor are they seen at lower particle volume fractions. Furthermore, the aggregates also do not form at pH 9 in the presence of TDA. Their production is therefore clearly a result of the presence of TAHP. The formation of TAHP occurs only at the interface, suggesting that these aggregates form either at the interface and then desorb or that they form in the bulk after TAHP crystallites have desorbed.

Interestingly, even adding a very large number of particles to a TAHP-stabilized emulsion does not greatly affect the droplet size. The light micrographs in Figure 5b show droplets of approximately the same size for all ϕ. Ostensibly, rather than stabilizing a greater amount of oil−water surface area, the colloidal PMMA aggregates with TAHP and leads to the formation of thicker interfaces. We have no reason to believe this is because the droplet size is limited by surface tension at the given shear rate. We have stabilized water-in-dodecane emulsions using PMMA alone with a mean diameter of 50 μm at the same shear rate (Figure S1a), a system for which one expects the surface tension to be that of a bare dodecane−water interface.[35] There are two possible reasons that the TAHP/PMMA-stabilized droplets are not significantly smaller than we observe. First, there may be weakly antagonistic interactions between the two stabilizers. It may be that the rate at which PMMA aggregates with TAHP is comparable to the rate at which droplet coalescence occurs, but then one would expect this to lead to antagonistic interactions under broader range of conditions (rather than just at ϕ_{high}). A second possibility is that the droplet size is shear-limited, but the limitation is the interfacial elasticity of the TAHP-PMMA network rather than the water−dodecane interfacial tension. The absence of thermal motion in the particles, along with the interfacial rheology measurements we have made in previous work,[24] shows that the TAHP film has an extremely large elastic modulus. We do not investigate this further here but note that the highly tunable nature of the TAHP film and the ability to dope the network with colloidal particles make for an interesting potential model system for the study of the mechanical properties of colloidal capsules. Future work could also consist of studying the conditions under which the drop size is limited by [TDA] and

DOI: 10.1021/acs.langmuir.6b01474
Langmuir 2016, 32, 6387−6397

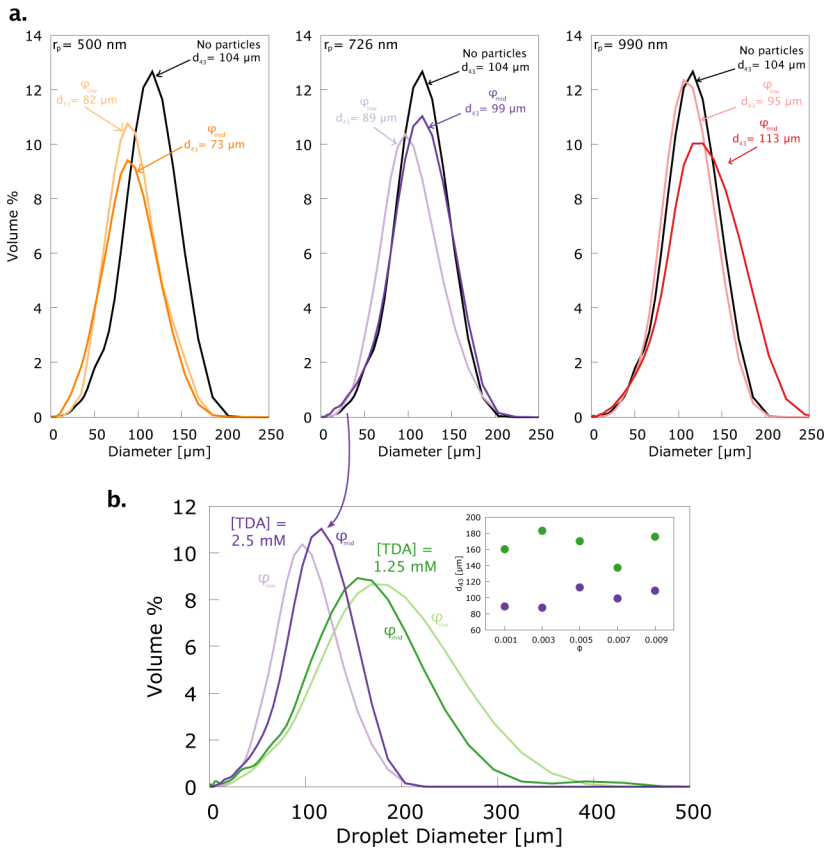

Figure 6. (a) Droplet size distributions obtained using static light scattering. Two different particle volume fractions (ϕ_{low}, light; ϕ_{mid}, dark; and none, black) were used. r_p = (l−r) 500, 726, 990 nm. (b) Droplet size distribution histogram for the emulsions containing a high (2.5 mM, purple) and a low (1.25 mM, green) concentration of TDA. r_p = 726 nm; light lines correspond to ϕ_{low} and dark lines correspond to ϕ_{high}. d_{43} values for the full ϕ range studied here are shown in the inset.

shear rate. This would allow for a controlled investigation into the importance of interfacial elasticity in emulsion processing.

[TDA] Determines Droplet Size at pH 5. We have argued that the results in Figure 2 demonstrate an increase in particle adsorption rate as the particle radius decreases. One possible confounding factor to our interpretation is that we may simply be adding an insufficient number of particles to make a significant impact on droplet size. In this section, we reduce [TDA] to 1.25 mM (giving droplets of roughly equal size to those formed at pH 7, [TDA] = 2.5 mM) and show that droplet size is independent of ϕ at pH 5, regardless of [TDA].

Figure 6a shows droplet size distributions for emulsions with (colored lines) and without (black line) added particles. Two different particle volume fractions (ϕ_{low} and ϕ_{mid}) were used for all r_p values studied. Varying the volume fraction of particles within the range shown here has no effect on the droplet size. A slight reduction in droplet size is still seen for r_p = 500 nm. Interestingly, this effect is apparently independent of ϕ, suggesting that it is not a consequence of the greater amount of surface area that the particles can cover. Regardless, the effect is sufficiently small that it is not investigated further here.

Figure 6b shows the effect of varying [TDA] on the droplet size at varying ϕ. Both droplet diameter distributions and d_{43} values of the distributions (inset) are shown. These experiments were performed over a broader range of particle volume fractions (ϕ = 0.001, 0.003, 0.005, 0.007, and 0.009). The graph of d_{43} vs ϕ shows that the droplet diameter is independent of ϕ. In stark contrast, varying [TDA] at pH 5 has a very large effect on the droplet size. Doubling [TDA] leads to a 40% reduction in d_{43}, in reasonable agreement with the inverse proportionality of these variables for emulsions stabilized by TAHP alone, as shown in Figure 1.

Figure 6 shows that, at pH 5, the size of the droplets stabilized by the composite TAHP/PMMA interface is determined almost entirely by [TDA]. In agreement with the results obtained so far, adding colloidal PMMA does not serve to reduce droplet size by coating additional oil−water surface area. This produces an apparent contradiction: if increasing the concentration of one stabilizer (the TDA) reduces the droplet size, then why does increasing the concentration of the other (the PMMA particles) not have the same effect? There are a number of possible reasons for this. First, it has been shown that additional particles increase the quantity of particles both at the interface and in the supernatant. Indeed, at very high particle volume fractions aggregates can be seen to protrude from the interface. This suggests that increasing the particle volume fraction acts to increase the thickness of the interface rather than stabilize more interfacial area. This does not, however, explain why changing [TDA] is then the only variable that determines the droplet size. The pH-dependent synergy between the particles shown in Figure 2 does, however, suggest a possible explanation. Clearly, when the TAHP-formation kinetics are significantly slowed, additional particles can lead to smaller droplets. Furthermore, we have shown that the droplet size at the shear rate used here is not surface-tension-limited. (See Figure S1, in which we stabilize 50 μm droplets at ϕ_{high} in the absence of TAHP.) This suggests that droplet breakup is inhibited in this system by interfacial elasticity. It also suggests

DOI: 10.1021/acs.langmuir.6b01474
Langmuir 2016, 32, 6387−6397

that the time scale on which the interfacial elasticity emerges determines the extent to which TAHP and PMMA can act synergistically.

The tuning of the interfacial density of particles as shown in Figure 5, combined with a drop size that can be tuned independently of particle volume fraction, also points to several applications. Most obviously, given the right conditions (pH of approximately 5, [TDA] $\geq$ 1 mM), this composite interface system allows us to fabricate rather large volumes of droplets with a controlled range of particle area density and droplet diameter. The composite interface consists of one component that is temperature-responsive that can be dissolved off (TAHP) and one component that is not (PMMA). Dissolution of the TAHP ought to to lead to the mobilization of the colloidal particles. The tunable particle density and droplet radius ought to give us access to a broader range of parameter space than has been studied for spherically confined two-dimensional colloidal dispersions thus far.

CONCLUSIONS

The size dependence of particle adsorption rates in a water-in-oil Pickering emulsion has been demonstrated. This was achieved by using a second, interfacially assembling emulsifier that inhibits particle adsorption at a tunable rate. The adsorption rate of the particles was altered by varying the particle radius (particle radii or 500, 726, and 990 nm were used), and the rate at which the TAHP film assembled was tuned by increasing the pH from 5 to 7.

Varying these two time scales leads to three regimes. At pH 5, when TAHP forms most rapidly, the addition of colloidal particles affects only the structure of the droplet interface, leaving the droplet size unaltered. At pH 7, when TAHP formation kinetics have been greatly retarded, the addition of colloidal PMMA leads to a reduction in droplet size, which systematically depends on the particle radius. The large, more slowly adsorbing particles lead to only a slight reduction in droplet size. The smaller, more rapidly adsorbing particles lead to a significantly greater reduction in droplet size. At pH 9, once TAHP is rendered inactive as a stabilizer, only the particles contribute to the droplet stability and Pickering emulsions are formed.

At pH 5, the system can be used to vary the area density of particles on the droplet without changing the droplet size. This has been shown to be the case for the full range of particle sizes studied here. We have also shown that droplet size can be easily tuned by varying the TDA concentration. In our previous work,[24] we noted that TAHP is temperature-responsive and can be dissolved off of the droplet by heating the system. This leads to the rheological moduli of a TAHP film being reduced to negligible values. We have performed preliminary work that shows that the PMMA particles remain attached to the interface after TAHP has been dissolved and that this results in the particles becoming mobile at the interface. The system we present here therefore has enormous potential for studying a number of colloidal phenomena confined to a sphere while giving access to a range of parameter space that has remained unexplored until now.

ASSOCIATED CONTENT

Supporting Information

The Supporting Information is available free of charge on the ACS Publications website at DOI: 10.1021/acs.langmuir.6b01474.

PMMA-stabilized Pickering emulsions, Composite interface structure at a range of particle radii, and derivation of the scaling of droplet size with particle radius (PDF)

AUTHOR INFORMATION

Corresponding Author

*E-mail: joe.forth@physics.org.

Notes

The authors declare no competing financial interest.

ACKNOWLEDGMENTS

We thank Andrew Schofield for synthesizing the PMMA particles and David French for useful discussions. J.F. was supported by a DRINC Scheme Studentship (BB/J50094/1).

REFERENCES

(1) Ramsden, W. Separation of Solids in the Surface-Layers of Solutions and 'Suspensions' (Observations on Surface-Membranes, Bubbles, Emulsions, and Mechanical Coagulation). - Preliminary Account. *Proc. R. Soc. London* **1903**, *72*, 156−164.

(2) Pickering, S. U. Emulsions. *J. Chem. Soc., Trans.* **1907**, *91*, 2001−2021.

(3) Binks, B. P.; Murakami, R. Phase inversion of particle-stabilized materials from foams to dry water. *Nat. Mater.* **2006**, *5*, 865−9.

(4) Tavacoli, J.; Katgert, G.; Kim, E.; Cates, M.; Clegg, P. Size Limit for Particle-Stabilized Emulsion Droplets under Gravity. *Phys. Rev. Lett.* **2012**, *108*, 268306.

(5) *Colloidal Particles at Liquid Interfaces*; Binks, B. P., Horozov, T. S., Eds.; Cambridge University Press: Cambridge, 2006; Chapter 1.

(6) Dickinson, E. Food emulsions and foams: Stabilization by particles. *Curr. Opin. Colloid Interface Sci.* **2010**, *15*, 40−49.

(7) Förster, T.; von Rybinski, W. In *Modern Aspects of Emulsion Science*; Binks, B. P., Ed.; Royal Society of Chemistry: Cambridge, 1998; Chapter 12.

(8) Stratford, K.; Adhikari, R.; Pagonabarraga, I.; Desplat, J.-C.; Cates, M. E. Colloidal jamming at interfaces: a route to fluid-bicontinuous gels. *Science* **2005**, *309*, 2198−2201.

(9) Suzuki, D.; Tsuji, S.; Kawaguchi, H. Janus microgels prepared by surfactant-free pickering emulsion-based modification and their self-assembly. *J. Am. Chem. Soc.* **2007**, *129*, 8088−8089.

(10) Chen, L.; Yu, S.; Wang, H.; Xu, J.; Liu, C.; Chong, W. H.; Chen, H. General methodology of using oil-in-water and water-in-oil emulsions for coiling nanofilaments. *J. Am. Chem. Soc.* **2013**, *135*, 835−843.

(11) Lopetinsky, R. J. G.; Masliyah, J. H.; Xu, Z. In *Colloidal Particles at Liquid Interfaces*; Binks, B. P., Horozov, T. S., Eds.; Cambridge University Press: Cambridge, 2006; Chapter 6.

(12) Tcholakova, S.; Denkov, N. D.; Lips, A. Comparison of solid particles, globular proteins and surfactants as emulsifiers. *Phys. Chem. Chem. Phys.* **2008**, *10*, 1608−1627.

(13) Davies, J. T. Turbulence phenomena at free surfaces. *AIChE J.* **1972**, *18*, 169−173.

(14) Collins, G. L.; Jameson, G. J. Double-layer effects in the of fine particles flotation. *Chem. Eng. Sci.* **1977**, *32*, 239−246.

(15) Ramirez, J. A.; Davis, R. H.; Zinchenko, A. Z. Microflotation of fine particles in the presence of a bulk-insoluble surfactant. *Int. J. Multiphase Flow* **2000**, *26*, 891−920.

(16) Nguyen, A. V.; Pugh, R. J; Jameson, G. J. In *Colloidal Particles at Liquid Interfaces*; Binks, B. P., Horozov, T. S., Eds.; Cambridge University Press: Cambridge, 2006; Chapter 9.

(17) Dai, Z.; Fornasiero, D.; Ralston, J. Particle-bubble collision models-a review. *Adv. Colloid Interface Sci.* **2000**, *85*, 231−256.

(18) Reay, D.; Ratcliff, G. A. Removal of fine particles from water by dispersed air flotation: Effects of bubble size and particle size on collection efficiency. *Can. J. Chem. Eng.* **1973**, *51*, 178−185.

DOI: 10.1021/acs.langmuir.6b01474
Langmuir 2016, 32, 6387−6397

(19) Nguyen, A. V.; George, P.; Jameson, G. J. Demonstration of a minimum in the recovery of nanoparticles by flotation: Theory and experiment. *Chem. Eng. Sci.* **2006**, *61*, 2494−2509.
(20) Deleurence, R.; Parneix, C.; Monteux, C. Mixtures of latex particles and the surfactant of opposite charge used as interface stabilizers - influence of particle contact angle, zeta potential, flocculation and shear energy. *Soft Matter* **2014**, *10*, 7088−7095.
(21) Walstra, P.; Smulders, P. E. A In *Modern Aspects of Emulsion Science*; Binks, B. P., Eds.; Royal Society of Chemistry: Cambridge, 1998; Chapter 2.
(22) Pichot, R.; Spyropoulos, F.; Norton, I. T. Mixed-emulsifier stabilised emulsions: Investigation of the effect of monoolein and hydrophilic silica particle mixtures on the stability against coalescence. *J. Colloid Interface Sci.* **2009**, *329*, 284−291.
(23) Thijssen, J. H. J.; Schofield, A. B.; Clegg, P. S. How do (fluorescent) surfactants affect particle-stabilized emulsions? *Soft Matter* **2011**, *7*, 7965.
(24) Forth, J.; French, D. J.; Gromov, A. V.; King, S.; Titmuss, S.; Lord, K. M.; Ridout, M. J.; Wilde, P. J.; Clegg, P. S. Temperature- and pH-Dependent Shattering: Insoluble Fatty Ammonium Phosphate Films at Water-Oil Interfaces. *Langmuir* **2015**, *31*, 9312−9324.
(25) Bosma, G.; Pathmamanoharan, C.; de Hoog, E. H. a.; Kegel, W. K.; van Blaaderen, A.; Lekkerkerker, H. N. W. Preparation of monodisperse, fluorescent PMMA-latex colloids by dispersion polymerization. *J. Colloid Interface Sci.* **2002**, *245*, 292−300.
(26) Campbell, A.; Bartlett, P. Fluorescent Hard-Sphere Polymer Colloids for Confocal Microscopy. *J. Colloid Interface Sci.* **2002**, *256*, 325−330.
(27) Ghosh, P. B.; Whitehouse, M. W. 7-Chloro-4-nitrobenzo-2-oxa-1,3-diazole: a New Fluorigenic Reagest for Amino Acids and other Amines. *Biochem. J.* **1968**, *108*, 155−156.
(28) Peters, R. A. Interfacial Tension and Hydrogen-Ion Concentration. *Proc. R. Soc. London, Ser. B* **1931**, *109*, 88−90.
(29) Betts, J. J.; Pethica, B. A. The ionization characteristics of monolayers of weak acids and bases. *Trans. Faraday Soc.* **1956**, *52*, 1581.
(30) Whitby, C. P.; Fischer, F. E.; Fornasiero, D.; Ralston, J. Shear-induced coalescence of oil-in-water Pickering emulsions. *J. Colloid Interface Sci.* **2011**, *361*, 170−7.
(31) Brenner, H. The slow motion of a sphere through a viscous fluid towards a plane surface. *Chem. Eng. Sci.* **1961**, *16*, 242−251.
(32) Ramirez, J. A.; Zinchenko, A.; Loewenberg, M.; Davis, R. H. The flotation rates of fine spherical particles under Brownian and convective motion. *Chem. Eng. Sci.* **1999**, *54*, 149−157.
(33) Schaaf, P.; Talbot, J. Surface exclusion effects in adsorption processes. *J. Chem. Phys.* **1989**, *91*, 4401−4409.
(34) French, D. J.; Taylor, P.; Fowler, J.; Clegg, P. S. Making and breaking bridges in a Pickering emulsion Making and breaking bridges in a Pickering emulsion. *J. Colloid Interface Sci.* **2015**, *441*, 30−38.
(35) Clegg, P. S.; Herzig, E. M.; Schofield, A. B.; Egelhaaf, S. U.; Horozov, T. S.; Binks, B. P.; Cates, M. E.; Poon, W. C. K. Emulsification of partially miscible liquids using colloidal particles: Nonspherical and extended domain structures. *Langmuir* **2007**, *23*, 5984−5994.

DOI: 10.1021/acs.langmuir.6b01474
Langmuir 2016, 32, 6387−6397